Oncology Research, Vol. 24, pp. 55–64
Printed in the USA.

0965-0407/16 $90.00 + .00
DOI: http://dx.doi.org/10.3727/096504016X14586627440192
E-ISSN 1555-3906
www.cognizantcommunication.com

2-Deoxy-D-glucose Suppresses the In Vivo Antitumor Efficacy of Erlotinib in Head and Neck Squamous Cell Carcinoma Cells

Arya Sobhakumari,*[1] Kevin P. Orcutt,†‡[1] Laurie Love-Homan,§ Christopher E. Kowalski,†‡ Arlene D. Parsons,† C. Michael Knudson,†‡§¶ and Andrean L. Simons*†‡§¶

*Interdisciplinary Human Toxicology Program, The University of Iowa, Iowa City, IA, USA
†Department of Radiation Oncology, The University of Iowa, Iowa City, IA, USA
‡Roy J. and Lucille A. Carver College of Medicine, The University of Iowa, Iowa City, IA, USA
§Department of Pathology, The University of Iowa, Iowa City, IA, USA
¶Holden Comprehensive Cancer Center, The University of Iowa, Iowa City, IA, USA

Poor tumor response to epidermal growth factor receptor (EGFR) tyrosine kinase inhibitors (TKIs) is a significant challenge for effective treatment of head and neck squamous cell carcinoma (HNSCC). Therefore, strategies that may increase tumor response to EGFR TKIs are warranted in order to improve HNSCC patient treatment and overall survival. HNSCC tumors are highly glycolytic, and increased EGFR signaling has been found to promote glucose metabolism through various mechanisms. We have previously shown that inhibition of glycolysis with 2-deoxy-D-glucose (2DG) significantly enhanced the antitumor effects of cisplatin and radiation, which are commonly used to treat HNSCC. The goal of the current studies is to determine if 2DG will enhance the antitumor activity of the EGFR TKI erlotinib in HNSCC. Erlotinib transiently suppressed glucose consumption accompanied by alterations in pyruvate kinase M2 (PKM2) expression. 2DG enhanced the cytotoxic effect of erlotinib in vitro but reversed the antitumor effect of erlotinib in vivo. 2DG altered the N-glycosylation status of EGFR and induced the endoplasmic reticulum (ER) stress markers CHOP and BiP in vitro. Additionally, the effects of 2DG+erlotinib on cytotoxicity and ER stress in vitro were reversed by mannose but not glucose or antioxidant enzymes. Lastly, the protective effect of 2DG on erlotinib-induced cytotoxicity in vivo was reversed by chloroquine. Altogether, 2DG suppressed the antitumor efficacy of erlotinib in a HNSCC xenograft mouse model, which may be due to increased cytoprotective autophagy mediated by ER stress activation.

Key words: Epidermal growth factor receptor (EGFR); Head and neck squamous cell carcinoma (HNSCC); Erlotinib; 2-Deoxy-D-glucose (2DG); Endoplasmic reticulum (ER) stress; Autophagy

INTRODUCTION

The majority of head and neck squamous cell carcinoma (HNSCC) tumors upregulate epidermal growth factor receptor (EGFR) signaling, which is associated with cell proliferation, survival, motility, and poor clinical prognosis (1,2). Various drugs that inhibit EGFR signaling have been developed for cancer therapy such as monoclonal antibodies (e.g., cetuximab, panitumumab) and tyrosine kinase inhibitors (TKIs) that target the cytoplasmic tyrosine kinase domain (e.g., gefitinib, erlotinib, lapatinib) (3). While these agents have been effective in the treatment of non-small cell lung cancer (NSCLC), currently only cetuximab is FDA approved for use in HNSCC. However, response rates in HNSCC to cetuximab as a single agent are quite low (13%) and of limited duration (2–3 months) (4–6). Additionally, low response rates (4–11%) have been observed in clinical trials with the TKIs gefitinib and erlotinib in HNSCC patients (5,7). In contrast, EGFR TKIs appear to be quite effective against NSCLC tumors, but only in tumors that harbor sensitizing EGFR mutations (4,6), which are rare in HNSCC. Therefore, further characterizations of strategies that increase tumor response to EGFR TKIs are warranted in order to improve HNSCC patient treatment and overall survival.

HNSCC tumors are highly dependent on glucose metabolism for energy production and regulation of cell death (8). Increased EGFR signaling promotes glucose metabolism through various mechanisms including

[1]These authors provided equal contribution to this work.
Address correspondence to Andrean L. Simons, Ph.D., Assistant Professor, Department of Pathology, University of Iowa, 1161 Medical Laboratories, 500 Newton Road, Iowa City, IA 52242, USA. Tel: 319-384-4450; Fax: 319-335-8453; E-mail: andrean-simons@uiowa.edu

increased Akt-dependent glycolysis (9), stabilization of the SGLT1 glucose transporter (10,11), increased STAT3 signaling (via HIF1 and GLUT1) (12–15), and increased pyruvate kinase M2 (PKM2) activity (16). EGFR inhibition was shown to downregulate glycolysis accompanied by suppression of key glycolytic enzymes including hexokinase-II (HKII) and PKM2 (17). Glycolysis inhibition has been shown to selectively induce cancer cell death while sparing normal untransformed cells by increasing mitochondrial oxidative stress (18). Additionally, inhibition of glycolysis with 2-deoxy-D-glucose (2DG) significantly enhanced the antitumor effects of various drugs and chemotherapy agents including cisplatin and radiation, which are important components of standard of care therapy in HNSCC (19,20). The goal of the current studies is to determine if 2DG will enhance the antitumor activity of the EGFR TKI erlotinib in HNSCC cells in vitro and in vivo. Here we show that 2DG enhanced HNSCC tumor cell response to erlotinib in vitro but not in vivo and that endoplasmic reticulum (ER) stress induction of autophagy may be involved in the observed results in vivo.

MATERIALS AND METHODS

Cells and Culture Conditions

FaDu, Cal-27, and SCC-25 human HNSCC cells were obtained from the American Type Culture Collection (ATCC, Manassas, VA, USA). SQ20B HNSCC cells (21) were a gift from Dr. Anjali Gupta (Department of Radiation Oncology, The University of Iowa). FaDu, Cal-27, and SQ20B cells were maintained in Dulbecco's modified Eagle's medium (DMEM) containing 4 mM of L-glutamine, 1 mM of sodium pyruvate, 1.5 g/L of sodium bicarbonate, and 4.5 g/L of glucose with 10% fetal bovine serum (FBS; Hyclone, Logan, UT, USA). All HNSCC cell lines are EGFR positive and are sensitive to EGFR inhibitors. All cell lines were authenticated by the ATCC for viability (before freezing and after thawing), growth, morphology, and isoenzymology. Cells were stored according to the supplier's instructions and used over a course of no more than 3 months after resuscitation of frozen aliquots. Cultures were maintained in 5% CO_2 and air humidified in a 37°C incubator.

Drug Treatment

Erlotinib (ERL) was obtained from Cayman Chemical. 2DG and tunicamycin (TUN) were obtained from Sigma-Aldrich. D(+)-mannose (MAN) was obtained from Acros Organics. Salubrinal (SAL) was obtained from Tocris. Dimethyl sulfoxide (DMSO) or PBS was used as vehicle control. Drugs were added to cells at final concentrations of 5 μM of ERL, 20 mM of 2DG, 20 mM of MAN, 1 μM of SAL, and 1 μg/ml of TUN. The required volume of each drug was added directly to complete cell culture media on cells to achieve the indicated final concentrations.

Glucose Consumption

Glucose consumption was determined by measuring glucose concentration in the media before and 24, 48, and 72 h post-drug treatment using a Bayer Ascensia™ Elite Glucometer with Bayer Ascensia Elite Blood glucose test strips. The amount of glucose consumed was normalized to cell number.

Reverse Transcriptase-Polymerase Chain Reaction

Total RNA was extracted from treated cells after indicated time points using the RNeasy mini kit (Qiagen). The cDNA was amplified from 800 ng of total RNA using iScript cDNA synthesis kit (Bio-Rad). Thermocycler conditions included a 5-min incubation at 25°C, a 30-min incubation at 42°C, and a 5-min incubation at 85°C. The cDNAs were subjected to qPCR analysis with the following 5′→3′ primers (sense and antisense, respectively): human PKM2: GCTGCAGTGGGGCCATAATCGT and CCTC GGGCCTTGCCAACATTCA, and human 18S: CCTTG GATGTGGTAGCCGTTT and AACTTTCGATGGTAGT CGCCG. The assay was performed in a 96-well optical plate, with a final reaction volume of 20 μl, including synthesized cDNA (20 ng), oligonucleotide primers (100 μM each), and 2× SYBR Green/ROX PCR master mix (Bio-Rad). Samples were run on an ABI PRISM Sequence Detection System (model 7000; Applied Biosystems). PCR conditions were 50°C for 2 min, 95°C for 2 min and 30 s, 95°C for 15 s, and 60°C for 1 min for 40 cycles. Results were analyzed using ABI PRISM 7000 SDS software. The denaturation and annealing steps were carried out for 40 cycles to determine the threshold cycle (CT) values for all of the genes analyzed. Samples were checked for nonspecific products or primer/dimer amplification by melting curve analysis. The CT values for the target genes in all of the samples (analyzed in duplicate or triplicate) were normalized on the basis of the abundance of the 18S transcript, and the fold difference (relative abundance) was calculated using the formula $2-\Delta\Delta CT$ and was plotted as the mean.

Western Blot Analysis

Cell lysates were standardized for protein content, resolved on 4% to 12% SDS polyacrylamide gels, and blotted onto nitrocellulose membranes. Membranes were probed with rabbit anti-pPKM2, anti-PKM2, anti-CHOP, anti-GRP78/BIP, anti-pEGFR (Y1086), anti-EGFR, anti-LC3B-I/II, and anti-β-actin (Cell Signaling). Antibody binding was detected by using an ECL Chemiluminescence Kit (Thermo Scientific).

Cell Survival Assays

HNSCC cells were seeded in a 96-well plate (2×10^3 cells/well) and incubated overnight under standard cell culture conditions (i.e., 95% relative humidity, 37°C, and 5% CO_2) before treating them with indicated drugs

for 48 h. Cell viability was measured by incubating with Prestoblue™ cell viability reagent (Invitrogen, USA) for 20 min at 37°C according to the manufacturer's protocol. Clonogenic survival was determined as previously described (22). Individual assays were performed with multiple dilutions with at least four cloning dishes per data point, repeated in at least three separate experiments.

Tumor Cell Implantation

Female 4- to 5-week-old athymic nu/nu nude mice were purchased from Harlan Laboratories (Indianapolis, IN, USA). Mice were housed in a pathogen-free barrier room in the Animal Care Facility at the University of Iowa and handled using aseptic procedures. All procedures were approved by the IACUC committee of the University of Iowa and conformed to the guidelines established by the NIH. Mice were allowed at least 3 days to acclimate prior to beginning experimentation, and food and water were made freely available. Tumor cells were inoculated into nude mice by subcutaneous injection of 0.1-ml aliquots of saline containing 4×10^6 FaDu cells into the right flank using 26-gauge needles.

Tumor Measurements

Mice started drug treatment 1 week after tumor inoculation. Mice were evaluated daily, and tumor measurements were taken three times per week using Vernier calipers. Tumor volumes were calculated using the formula: tumor volume = (length × width^2)/2, where the length was the longest dimension, and the width was the dimension perpendicular to length.

In Vivo Drug Administration

2DG was obtained from Sigma-Aldrich and dissolved in water. Erlotinib (Tarceva) was obtained from the pharmacy at the University of Iowa Hospitals and Clinics and suspended in water before administration. Mice were divided into four groups ($n = 6$ mice/group). ERL group: ERL was suspended in water and administered orally 12.5 mg/kg every day for 2 weeks; 2DG group: 2DG was administered IP 500 mg/kg every day for 2 weeks; ERL + 2DG group: mice were administered ERL orally 12.5 mg/kg and 500 mg/kg 2DG IP every day for 2 weeks; control group: mice were administered orally and IP 100 µl water every day for 2 weeks. Mice were euthanized via CO_2 gas asphyxiation when tumor diameter exceeded 1.5 cm in any dimension.

Statistical Analysis

Statistical analysis was done using GraphPad Prism version 5 for Windows (GraphPad Software, San Diego, CA, USA). Differences between three or more means were determined by one-way ANOVA with Tukey post-tests. Linear mixed effects regression models were used to estimate and compare the group-specific change in tumor growth curves. All statistical analyses were performed at the $p < 0.05$ level of significance.

RESULTS

Erlotinib Transiently Affects Glucose Consumption in HNSCC Cells

The effect of ERL on glucose consumption of HNSCC cells was determined by treating FaDu, Cal-27, SCC25, and SQ20B cell lines with a clinically relevant dose of 5 µM of ERL (23) and measuring the amount of glucose consumed in the media per cell after 24 h. ERL significantly decreased glucose consumption after 24 h in all HNSCC cells compared to the DMSO-treated control cells (Fig. 1A). To investigate if this decrease in glucose consumption was associated with a change in expression of PKM2, which is known to be essential for glucose metabolism in tumor cells (14), SCC25 cells were treated with ERL for 24 and 48 h, and the relative mRNA and protein levels were assessed. ERL significantly decreased mRNA (Fig. 1B) and protein (Fig. 1C) expression of PKM2 at both 24 and 48 h, suggesting that ERL may decrease glucose consumption and glycolysis by suppressing PKM2 expression. Surprisingly, the initial suppression of glucose consumption by ERL after 24 h (Fig. 1A) was not retained after 48 h, and glucose levels were fully restored after 72 h (Fig. 1D). Additionally, ERL treatment induced significant cytotoxicity after 24 h with no further increase in cytotoxicity after 48 and 72 h of treatment, which supports our prior results (24) showing the rapid development of ERL drug tolerance in these cell lines. Altogether, these results indicate that ERL transiently suppresses glucose consumption and suggests a compensatory mechanism may be involved in the restoration of glucose consumption rates despite the presence of ERL.

2DG Enhances the Efficacy of ERL In Vitro but not In Vivo

To determine if the efficacy of ERL can be enhanced by inhibiting glucose uptake, HNSCC cells were treated with the glycolytic inhibitor 2DG with or without ERL and analyzed for clonogenic survival. 2DG at 20 mM was chosen for the current studies to ensure that a physiologically relevant ratio of 2DG/glucose (ratio 0.8) was used to inhibit glucose metabolism in the HNSCC cells grown in DMEM that contained 25 mM of glucose (25). 2DG significantly enhanced the in vitro cytotoxicity of ERL in FaDu and Cal-27 cells but not SCC-25 cells (Fig. 2A). In the SQ20B cell line, 2DG as a single agent was equally as effective as 2DG + ERL (Fig. 2A). The in vivo activity of 2DG and ERL in FaDu tumor-bearing athymic nude nice was examined. The results showed that the administration of ERL significantly suppressed tumor growth compared to the control as expected; however, 2DG did not enhance

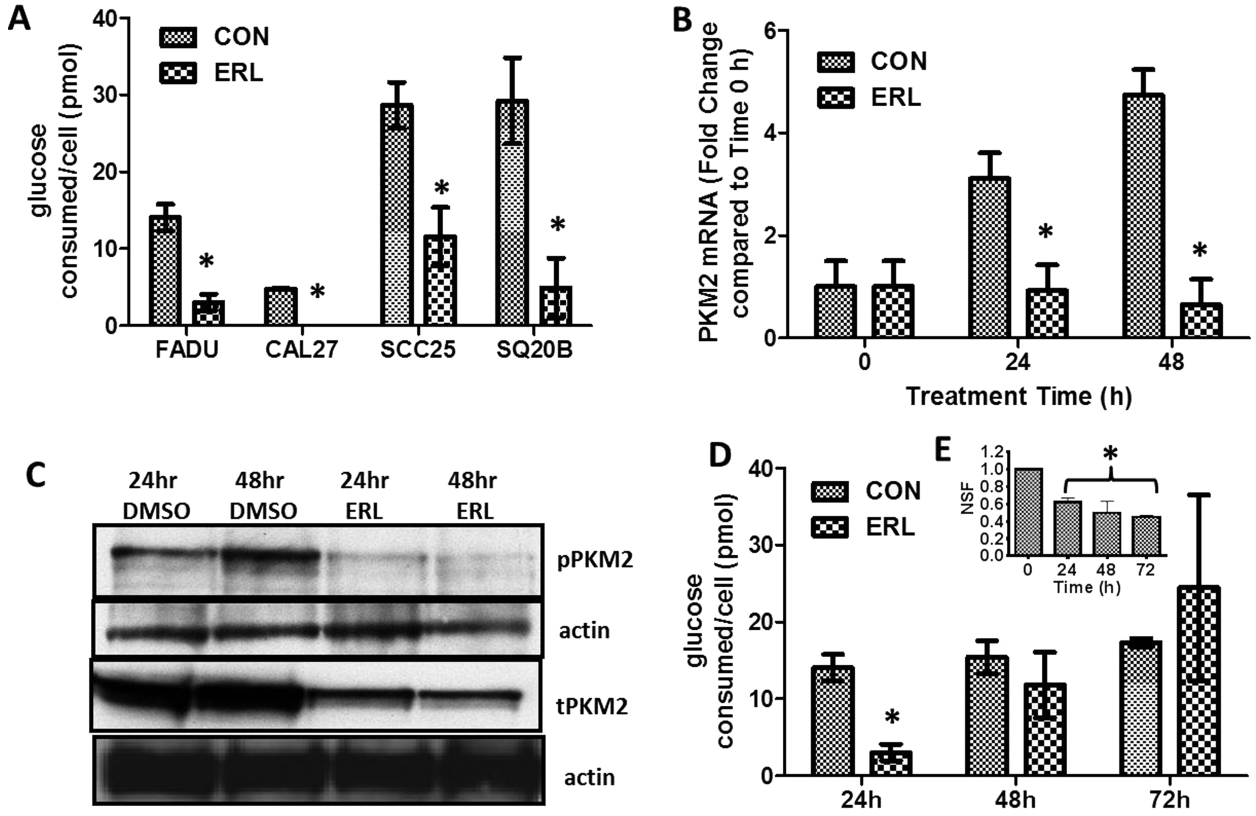

Figure 1. Erlotinib suppresses glucose consumption in HNSCC cells. (A) Glucose concentrations in the cell culture media of FaDu, Cal-27, SCC-25, and SQ20B HNSCC cells were measured before and after 24 h DMSO (CON) or erlotinib (ERL) treatment. (B, C) SCC-25 cells were treated with DMSO or ERL for 24 and 48 h then analyzed for PKM2 mRNA levels by RT-PCR (B) and protein levels by Western blot (C). (D, E) FaDu cells were treated with DMSO or ERL, and glucose concentrations (D) and clonogenic survival (E) were measured 24, 48, and 72 h after treatment. Glucose concentrations were normalized to cell number. NSF, normalized surviving fraction. Error bars represent ± standard error of the mean (SEM) of at least $N = 3$ experiments. *$p < 0.05$ versus DMSO.

the antitumor activity of ERL (Fig. 2B). Surprisingly, 2DG suppressed the antitumor activity of ERL as shown by the 2DG+ERL-treated tumors growing at a similar rate to the control-treated tumors (Fig. 2B). The combination of 2DG+ERL also did not significantly increase the median survival of the mice compared to the other treatment groups [14.5 days (2DG+ERL) vs. 8.5 (CON), 10 (2DG), 11.5 (ERL) days] (Fig. 2C). These results suggested that 2DG enhances the efficacy of ERL in vitro but not in vivo.

2DG Induces Markers of ER Stress

2DG has been previously reported to not only inhibit glucose metabolism but also induce ER stress through inhibition of protein glycosylation, which contributes to the toxicity of 2DG in vitro (26–28). To determine if ER stress was playing a role in the effects of 2DG and/or ERL, we initially investigated changes in the expression of the ER stress markers CHOP and GRP78 in response to drug treatment in FaDu, Cal-27, and SQ20B cells (Fig. 3). The SCC-25 cell line was excluded for the remainder of these studies since 2DG did not enhance ERL-induced cytotoxicity in this cell line (Fig. 2A). In Cal-27 and SQ20B, 2DG+ERL treatment increased the expression of CHOP (Fig. 3A) and GRP78 (Fig. 3B), which was comparable to that of tunicamycin (positive control). In FaDu cells, 2DG+ERL treatment induced both CHOP (Fig. 3A) and GRP78 (Fig. 3B); however, 2DG and ERL treatment alone also increased GRP78 expression (Fig. 3B). Pretreatment of all cell lines with MAN, an agent that blocks 2DG-induced ER stress without affecting its inhibition of glycolysis, reversed CHOP and GRP78 expression that was induced by 2DG and 2DG+ERL (Figure 3A, B), suggesting that 2DG+ERL treatment increases ER stress in HNSCC cells.

Suppression of ER Stress Reverses Drug-Induced Cell Killing

To determine if ER stress was involved in 2DG+ERL-induced cell killing, FaDu, Cal-27, and SQ20B cell lines were pretreated with 20 mM of MAN for 2 h before 2DG+ERL treatment and analyzed for changes in cell viability. MAN significantly rescued Cal-27 and SQ20B

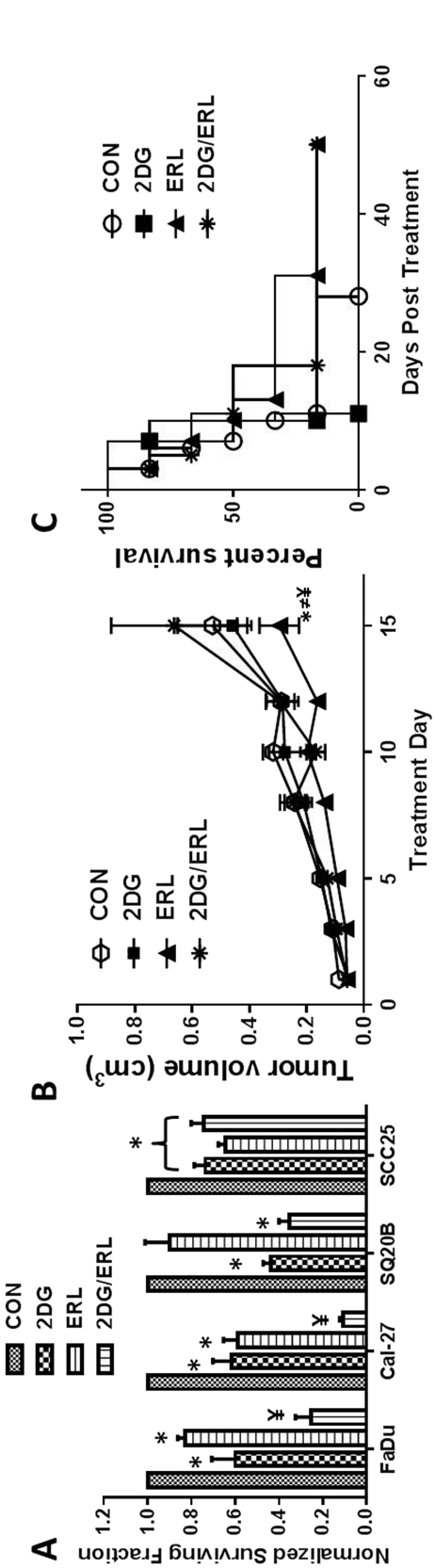

Figure 2. 2-Deoxy-D-glucose (2DG) enhances the antitumor efficacy of erlotinib in vitro but not in vivo. (A) FaDu, Cal-27, SCC25, and SQ20B cells were treated with 2DG with or without erlotinib (ERL) and analyzed for cell survival by clonogenic assay. Error bars represent ± standard error of the mean (SEM) of at least $N = 3$ experiments. $*p < 0.05$ versus DMSO, ¥$p < 0.05$ versus 2DG/ERL. (B) FaDu cells were injected into the right flank of athymic nu/nu mice ($n = 6$) and treated with 2DG alone or in combination with ERL for 2 weeks. Saline was administered as a control (CON). Tumor growth was measured using Vernier calipers. (C) Kaplan–Meier plot of survival data. $*p < 0.05$ ERL versus CON, ≠$p < 0.05$ ERL versus 2DG, ¥$p < 0.05$ ERL versus 2DG/ERL.

cells (but not FaDu) from 2DG + ERL-induced cell killing (Fig. 4A). However, when FaDu cells were further analyzed using a clonogenic assay, we observed that MAN significantly rescued FaDu cells from 2DG + ERL-induced cytotoxicity (Fig. 4B). The ER stress suppressor SAL, which is a selective inhibitor of eukaryotic translation initiation factor 2 subunit α (eIF2α) dephosphorylation, also significantly rescued FaDu cells from 2DG + ERL-induced cytotoxicity (Fig. 4B), suggesting that ER stress may be responsible for the 2DG + ERL-induced cytotoxicity observed in vitro (Fig. 3A).

2DG Alters EGFR Expression

Given that N-linked glycosylation is important for EGFR expression and activity (29,30) and 2DG is known to induce ER stress by inhibition of N-linked glycosylation (27), we determined if 2DG altered the expression of EGFR in FaDu, Cal-27, and SQ20B cells. Using FaDu cells, we showed that ERL decreased the phosphorylation of EGFR and its downstream pathway protein Akt as expected (Fig. 5A). However, 2DG and 2DG + ERL resulted in the separation of the total (unphosphorylated) EGFR band, accumulation of a smaller sized EGFR (~150 kDa), and decreased amounts of the full-length EGFR (170 kDa) compared to the control (Fig. 5A). 2DG caused a similar effect to the phosphorylated EGFR (pEGFR) band compared to the control but, more importantly, 2DG + ERL completely inhibited EGFR phosphorylation even more so than ERL alone (Fig. 5A). Similar results with respect to phosphorylated EGFR were observed in Cal-27 and SQ20B cells (data not shown). We further analyzed the potential effects of 2DG with or without ERL on EGFR glycosylation by resolving the cell lysates from drug-treated cells for 15 min longer (1 h vs. 45 min) to allow for further separation of the EGFR bands (Fig. 5B, C). Again, 2DG + ERL partially or completely suppressed expression of the full-length EGFR compared to the control or ERL-treated cells in all cell lines (Fig. 5B, C). However 2DG + ERL also increased the expression of two smaller EGFR bands at around 150 and 140 kDa (Fig. 5B, C) depending on the cell line analyzed. FaDu cells appeared to express the 140-kDa band in all treatment groups (Fig. 5B, C). The observed changes in EGFR expression induced by 2DG + ERL were reversed by pretreatment with MAN, suggesting that ER stress may be involved. Tunicamycin (positive control)-treated cells dramatically decreased the expression of the 170-kDa band and consistently induced the expression of the smaller 140-kDa band in all cell lines (Fig. 5C). Altogether these results suggest that 2DG + ERL alters EGFR expression by disrupting EGFR N-linked glycosylation and ER stress.

2DG and ERL Induce Autophagy

Various studies have previously shown that autophagy can act as a prosurvival mechanism when stimulated by

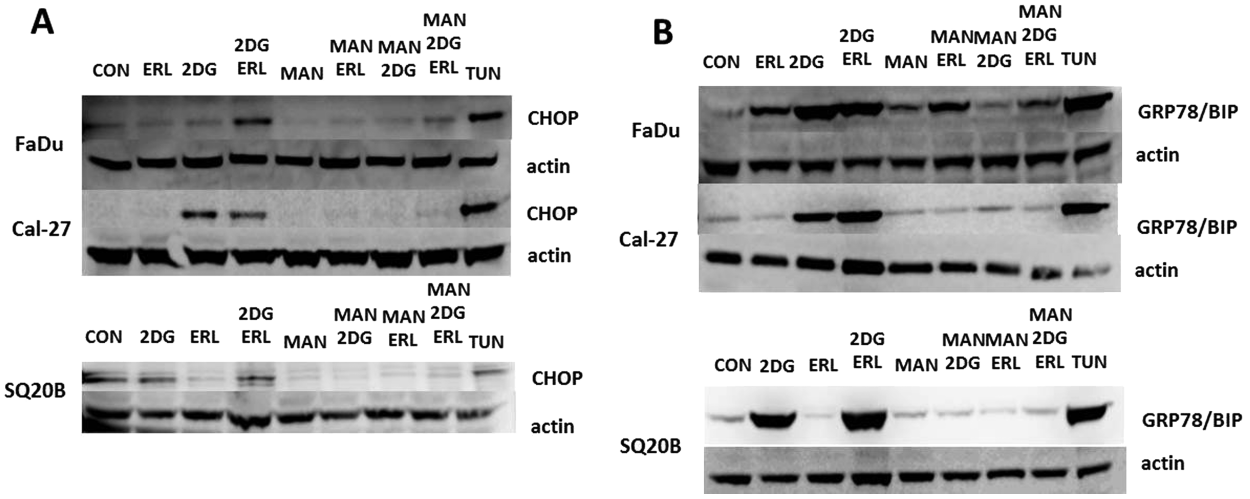

Figure 3. 2-Deoxy-D-glucose (2DG) induces markers or ER stress. (A) FaDu, Cal-27, and SQ20B cells were pretreated with mannose (MAN) for 2 h before treatment with 2DG and/or ERL then analyzed for CHOP (A) and GRP78/BIP (B) expression. Cells were treated with saline as a negative control (CON) and tunicamycin (TUN) as a positive control. β-Actin was used as a loading control.

stressful cellular conditions such as chemotherapy and ER stress (31–33). To determine if 2DG+ERL-induced ER stress activates autophagy, we analyzed the HNSCC cells for the conversion of the microtubule-associated protein light chain 3B (LC3B) from unconjugated LC3B-I to its lipidated form LC3B-II. 2DG and 2DG+ERL increased LC3B-II and/or LC3B-I compared to the other treatment groups, indicating the induction of autophagy (Fig. 6A). The observed drug-induced increases in LC3B-1/LC3B-II were suppressed when the cells were pretreated with MAN (Fig. 6A), suggesting that ER stress was responsible for autophagy induction. To investigate whether the decreased antitumor efficacy of 2DG+ERL in vivo was due to the induction of a protective autophagy mechanism, athymic nude mice bearing FaDu xenografts were treated with the autophagy inhibitor chloroquine (CLQ)

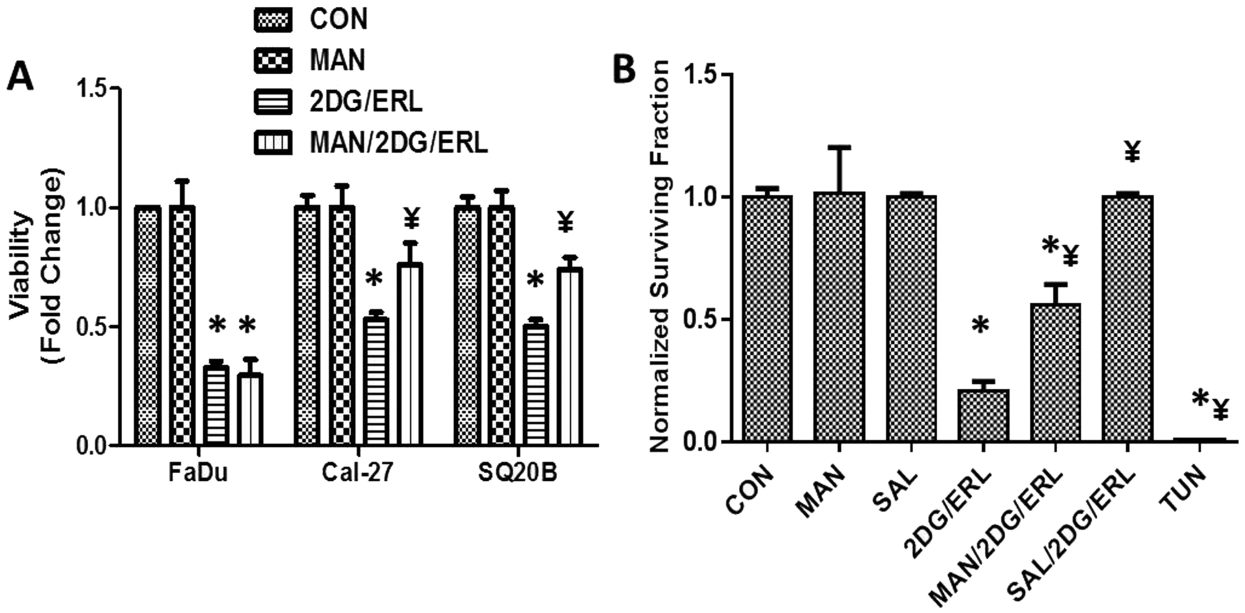

Figure 4. Suppression of ER stress reverses drug-induced cell killing. (A) FaDu, Cal-27, and SQ20B cells were pretreated with mannose (MAN) for 2 h before treatment with 2DG+ERL then analyzed for cell viability. (B) FaDu cells were pretreated with MAN or salubrinal (SAL) for 2 h before treatment with 2DG+ERL then analyzed for clonogenic survival. Cells were treated with saline as a control (CON). Error bars represent ± standard error of the mean (SEM) of at least $N=3$ experiments. *$p<0.05$ versus CON, ¥$p<0.05$ versus 2DG+ERL.

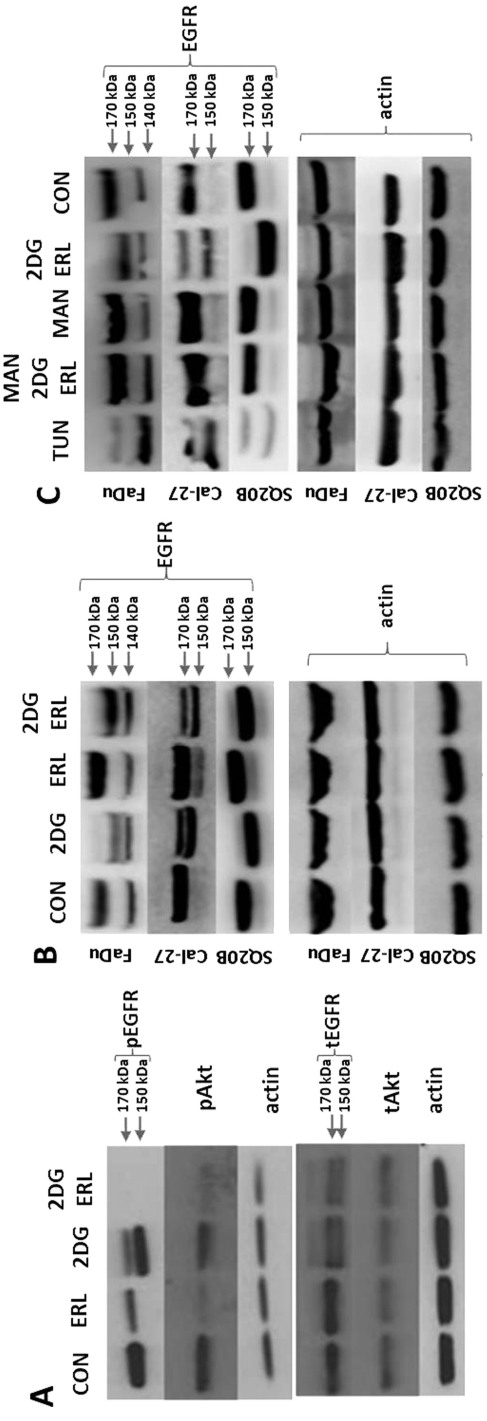

Figure 5. 2-Deoxy-D-glucose (2DG) alters EGFR expression. (A) FaDu cells were treated with 2DG with or without erlotinib (ERL) and analyzed for phosphorylated EGFR (pEGFR) and Akt (pAkt) expression and total EGFR (tEGFR) and Akt (tAkt) expression by Western blot. (B) FaDu, Cal-27, and SQ20B cells were treated with 2DG with or without ERL and analyzed for total EGFR (EGFR) expression. (C) FaDu, Cal-27, and SQ20B cells were pretreated with mannose (MAN) for 2 h before treatment with 2DG + ERL then analyzed for EGFR expression. Cells were treated with saline as a negative control (CON) and tunicamycin (TUN) as a positive control. β-Actin was used as a loading control.

alone or in combination with 2DG and/or ERL. This experiment was terminated at day 9 instead of day 15 as shown previously (Fig. 2B) because the tumors reached our euthanization criteria (1.5 cm in any direction) more rapidly than the prior experiment. For clarity, only the tumor volumes for each treatment group at day 9 are shown in Figure 6B. As demonstrated previously in Figure 2B, 2DG reversed the antitumor effect of ERL, and the growth of 2DG + ERL-treated tumors was not affected compared to the control (Fig. 6B). However, CLQ combined with 2DG + ERL demonstrated smaller tumor volumes at day 9 compared to CON-, CLQ-, and 2DG + ERL-treated tumors, suggesting that the autophagy may play a role in reducing the efficacy of 2DG + ERL (Fig. 6B). Overall, our data suggest that 2DG reduces the antitumor efficacy of ERL by inducing ER stress-mediated autophagy and that the use of glycolytic inhibitors in combination with EGFR inhibitors is not supported by our findings.

DISCUSSION

The relationship between EGFR and glucose metabolism has been previously established through various mechanisms (9–17). However, the finding that the suppression of glucose uptake by ERL treatment was transient and was restored by 48–72 h was not expected and implies that a compensatory mechanism may be involved. Additionally, ERL-induced cytotoxicity was significantly increased after 24 h but not after 48–72 h, suggesting that there may be some correlation between glucose consumption and drug tolerance. Glycolytic inhibition is known to induce autophagy, which is a self-degradation phenomenon activated under conditions of stress that acts as a cell survival or cell death mechanism depending on the cell type, stress type/duration, and other factors (27,34,35). We have previously shown that ERL induces cytoprotective autophagy after 48 and 72 h and that suppression of select autophagy genes could increase the efficacy of ERL in vitro (24). Perhaps intracellular glucose levels were restored after 48 h during the process of autophagy resulting in ERL drug tolerance. Furthermore, a study by Weihua et al. demonstrated that EGFR independent of its kinase activity can maintain basal intracellular glucose levels in the presence of low glucose conditions by interacting with the sodium/glucose transporter 1 (SGLT1), resulting in the prevention of autophagic cell death (11). Although this line of research is beyond the scope of this work, it is possible that ERL may induce the interaction between EGFR and SGLT1, which would explain the restoration of glucose levels observed in our HNSCC cells.

In an effort to prevent the restoration of glucose levels in the presence of ERL, 2DG, which is a known glycolytic inhibitor, was utilized to determine if this agent would sensitize HNSCC cells to ERL-induced cytotoxicity. 2DG mimics glucose deprivation because it competes

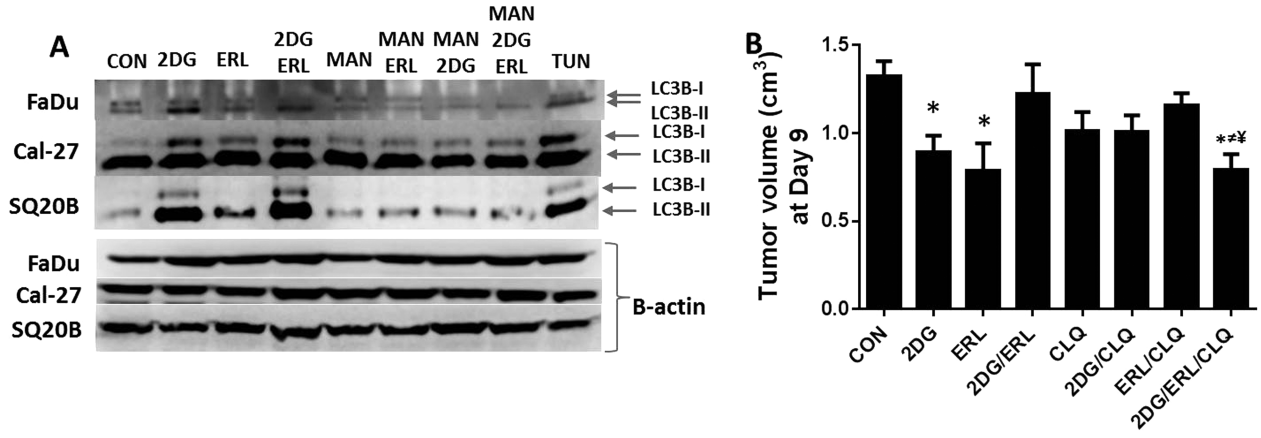

Figure 6. 2-Deoxy-D-glucose (2DG) and erlotinib (ERL) induce autophagy. (A) FaDu, Cal-27, and SQ20B cells were pretreated with mannose (MAN) for 2 h before treatment with 2DG and/or ERL then analyzed for LC3BI/II expression. Cells were treated with saline as a negative control (CON) and tunicamycin (TUN) as a positive control. β-Actin was used as a loading control. (B) FaDu cells were injected into the right flank of athymic nu/nu mice ($n=6$) and treated with 2DG in combination with ERL (2DG/ERL) with or without chloroquine (CLQ) for 9 days. Saline was administered as a control (CON). Tumor growth was measured using Vernier calipers. Error bars represent ± standard error of the mean (SEM) of $N=6$ mice. *$p<0.05$ versus CON, ≠$p<0.05$ versus CLQ, ¥$p<0.05$ versus 2DG/ERL.

with glucose for uptake by GLUT transporters into the cell, but is only able to undergo the first step in glycolysis (mediated by hexokinase) into its phosphorylated product: 2DG-6-phosphate (36). 2DG treatment results in a reduction in pyruvate and a deficiency in NADPH since 2DG-6-phosphate can only undergo the first step in the pentose phosphate pathway (PPP) to generate 2DG-6-phosphoglaconalactone and one molecule of NADPH from $NADP^+$, but cannot be metabolized further (36). As a result, 2DG increases oxidative stress by shifting from aerobic glycolysis to mitochondrial oxidative metabolism and suppressing antioxidant enzymes that depend on NADPH such as glutathione reductase and thioredoxin reductase (37). As mentioned before, our group has demonstrated previously that 2DG induces oxidative stress, leading to cell killing and sensitization of tumor cells to various chemotherapy agents and radiation in vitro and in vivo (19,20,38–40). Here we show that 2DG effectively enhanced the antitumor efficacy of ERL in the majority of our HNSCC cell lines; however, we were unable to detect any involvement of oxidative stress as measured by the percentage of oxidized glutathione (data not shown). Additionally, we were unable to rescue any of the observed cytotoxic effects induced by 2DG+ERL using antioxidant enzymes such as superoxide dismutase (SOD) and catalase (CAT) (data not shown).

A lesser known feature of 2DG is its role in ER stress, which is a process that occurs when there is a compromise in the protein folding capacity of the ER (27). Under conditions of cellular stress, including starvation, hypoxia, and defective protein degradation, ER stress may occur (41). As a result, misfolded proteins aggregate and signal the unfolded protein response (UPR) characterized by a reduction in global protein synthesis and synthesis of proteins involved in folding including the chaperone BiP/Grp78 (41). When ER stress is so extensive that the cell cannot restore homeostasis, the protein CHOP is upregulated, resulting in apoptotic cell death (41). Indeed, we observed that 2DG and 2DG+ERL induced the expression of both BiP/Grp78 and CHOP in our HNSCC cell lines (Fig. 3). MAN, which is the main sugar of the oligosaccharide chain in N-linked glycosylation, reversed 2DG+ERL-induced ER stress (Fig. 3) and cell death (Fig. 4), suggesting that ER stress, rather than oxidative stress or glycolytic inhibition, was associated with the observed effects. Due to 2DG's structural similarity to MAN, 2DG interferes with oligosaccharide synthesis, leading to abnormal N-linked glycosylation of proteins and resulting in ER stress (26,27). N-glycosylation is also an important characteristic of EGFR and is necessary for normal EGFR function such as conformation, ligand binding, and tyrosine kinase activity (42,43), which suggests that 2DG treatment would disrupt EGFR function and signaling. We saw that 2DG treatment altered the glycosylation status of EGFR in all cell lines tested, and it is likely that the glycosylation status of numerous other proteins was altered by 2DG treatment, leading to ER stress.

The finding that 2DG reversed, instead of enhanced, the cytotoxicity of ERL in vivo was another unexpected find. Other studies have shown that in NSCLC cells bearing a T790M mutation, which renders these cells resistant to reversible EGFR TKIs such as ERL and gefitinib, 2DG enhanced the effect in vivo of afatinib, which is a second-generation irreversible EGFR TKI that targets

the T790M mutation (44). Given this finding, it is possible that 2DG may overcome ERL resistance instead of enhancing ERL efficacy.

Although ER stress appeared to be responsible for 2DG+ERL-induced cell killing in vitro, ER stress may also induce autophagy, which may act as a protective mechanism in vivo in our cell model (34). In support of this, 2DG has been found to induce autophagy mediated by ER stress (and not glucose deprivation) (26,27). We observed that 2DG and 2DG+ERL did induce autophagy as observed by increased LC3BI/II expression compared to the other groups, and these effects were all reversed by MAN. We confirmed the possible mechanism of autophagy in vivo by showing that CLQ could reverse the effects of 2DG on ERL treatment. These findings illustrate the "double-edged sword" nature of ER stress in that ER stress was associated with drug-induced cell death in vitro; however, this same ER stress is able to induce cytoprotective autophagy in vivo. It is also possible that other unknown immune response mechanisms could be responsible for the vast difference in the in vitro and in vivo results. Nevertheless, based on these results, the use of 2DG as an adjuvant to ERL-based therapy is not supported by these studies.

ACKNOWLEDGMENTS: This work was supported by the Department of Pathology and National Institutes of Health (NIH) grants K01CA134941 and NIH R01DE024550, and IRG-77-004-34 from the American Cancer Society (ACS), administered through the Holden Comprehensive Cancer Center at the University of Iowa. The authors declare no conflicts of interest.

REFERENCES

1. Ang, K. K.; Berkey, B. A.; Tu, X.; Zhang, H. Z.; Katz, R.; Hammond, E. H.; Fu, K. K.; Milas, L. Impact of epidermal growth factor receptor expression on survival and pattern of relapse in patients with advanced head and neck carcinoma. Cancer Res. 62:7350–7356; 2002.
2. Grandis, J. R.; Tweardy, D. J. TGF-alpha and EGFR in head and neck cancer. J. Cell Biochem. Suppl. 17F:188–191; 1993.
3. Loeffler-Ragg, J.; Schwentner, I.; Sprinzl, G. M.; Zwierzina, H. EGFR inhibition as a therapy for head and neck squamous cell carcinoma. Expert Opin. Investig. Drugs 17:1517–1531; 2008.
4. Lynch, T. J.; Bell, D. W.; Sordella, R.; Gurubhagavatula, S.; Okimoto, R. A.; Brannigan, B. W.; Harris, P. L.; Haserlat, S. M.; Supko, J. G.; Haluska, F. G.; Louis, D. N.; Christiani, D. C.; Settleman, J.; Haber, D. A. Activating mutations in the epidermal growth factor receptor underlying responsiveness of non-small-cell lung cancer to gefitinib. N. Engl. J. Med. 350:2129–2139; 2004.
5. Sequist, L. V.; Bell, D. W.; Lynch, T. J.; Haber, D. A. Molecular predictors of response to epidermal growth factor receptor antagonists in non-small-cell lung cancer. J. Clin. Oncol. 25:587–595; 2007.
6. Vermorken, J. B.; Trigo, J.; Hitt, R.; Koralewski, P.; Diaz-Rubio, E.; Rolland, F.; Knecht, R.; Amellal, N.; Schueler, A.; Baselga, J. Open-label, uncontrolled, multicenter phase II study to evaluate the efficacy and toxicity of cetuximab as a single agent in patients with recurrent and/or metastatic squamous cell carcinoma of the head and neck who failed to respond to platinum-based therapy. J. Clin. Oncol. 25:2171–2177; 2007.
7. Piperdi, B.; Perez-Soler, R. Role of erlotinib in the treatment of non-small cell lung cancer: Clinical outcomes in wild-type epidermal growth factor receptor patients. Drugs 72(Suppl. 1):11–19; 2012.
8. Sandulache, V. C.; Ow, T. J.; Pickering, C. R.; Frederick, M. J.; Zhou, G.; Fokt, I.; Davis-Malesevich, M.; Priebe, W.; Myers, J. N. Glucose, not glutamine, is the dominant energy source required for proliferation and survival of head and neck squamous carcinoma cells. Cancer 117:2926–2938; 2011.
9. Makinoshima, H.; Takita, M.; Saruwatari, K.; Umemura, S.; Obata, Y.; Ishii, G.; Matsumoto, S.; Sugiyama, E.; Ochiai, A.; Abe, R.; Goto, K.; Esumi, H.; Tsuchihara, K. Signaling through the phosphatidylinositol 3-kinase (PI3K)/mammalian target of rapamycin (mTOR) axis is responsible for aerobic glycolysis mediated by glucose transporter in epidermal growth factor receptor (EGFR)-mutated lung adenocarcinoma. J. Biol. Chem. 290:17495–17504; 2015.
10. Ren, J.; Bollu, L. R.; Su, F.; Gao, G.; Xu, L.; Huang, W. C.; Hung, M. C.; Weihua, Z. EGFR-SGLT1 interaction does not respond to EGFR modulators, but inhibition of SGLT1 sensitizes prostate cancer cells to EGFR tyrosine kinase inhibitors. Prostate 73:1453–1461; 2013.
11. Weihua, Z.; Tsan, R.; Huang, W. C.; Wu, Q.; Chiu, C. H.; Fidler, I. J.; Hung, M. C. Survival of cancer cells is maintained by EGFR independent of its kinase activity. Cancer Cell 13:385–393; 2008.
12. Camporeale, A.; Demaria, M.; Monteleone, E.; Giorgi, C.; Wieckowski, M. R.; Pinton, P.; Poli, V. STAT3 activities and energy metabolism: Dangerous liaisons. Cancers (Basel) 6:1579–1596; 2014.
13. Demaria, M.; Camporeale, A.; Poli, V. STAT3 and metabolism: How many ways to use a single molecule? Int. J. Cancer 135:1997–2003; 2014.
14. Demaria, M.; Poli, V. PKM2, STAT3 and HIF-1alpha: The Warburg's vicious circle. Jakstat 1:194–196; 2012.
15. Demaria, M.; Giorgi, C.; Lebiedzinska, M.; Esposito, G.; D'Angeli, L.; Bartoli, A.; Gough, D. J.; Turkson, J.; Levy, D. E.; Watson, C. J.; Wieckowski, M. R.; Provero, P.; Pinton, P.; Poli, V. A STAT3-mediated metabolic switch is involved in tumour transformation and STAT3 addiction. Aging (Albany NY) 2:823–842; 2010.
16. Yang, W.; Xia, Y.; Cao, Y.; Zheng, Y.; Bu, W.; Zhang, L.; You, M. J.; Koh, M. Y.; Cote, G.; Aldape, K.; Li, Y.; Verma, I. M.; Chiao, P. J.; Lu, Z. EGFR-induced and PKCepsilon monoubiquitylation-dependent NF-kappaB activation upregulates PKM2 expression and promotes tumorigenesis. Mol. Cell 48:771–784; 2012.
17. De Rosa, V.; Iommelli, F.; Monti, M.; Fonti, R.; Votta, G.; Stoppelli, M. P.; Del Vecchio, S. Reversal of Warburg effect and reactivation of oxidative phosphorylation by differential inhibition of EGFR signaling pathways in non-small cell lung cancer. Clin. Cancer Res. 21:5110–5120; 2015.
18. Aykin-Burns, N.; Ahmad, I. M.; Zhu, Y.; Oberley, L. W.; Spitz, D. R. Increased levels of superoxide and H2O2 mediate the differential susceptibility of cancer cells versus normal cells to glucose deprivation. Biochem. J. 418:29–37; 2009.
19. Simons, A. L.; Fath, M. A.; Mattson, D. M.; Smith, B. J.; Walsh, S. A.; Graham, M. M.; Hichwa, R. D.; Buatti, J. M.; Dornfeld, K.; Spitz, D. R. Enhanced response of human head and neck cancer xenograft tumors to cisplatin combined

with 2-deoxy-D-glucose correlates with increased 18F-FDG uptake as determined by PET imaging. Int. J. Radiat. Oncol. Biol. Phys. 69:1222–1230; 2007.
20. Simons, A. L.; Ahmad, I. M.; Mattson, D. M.; Dornfeld, K. J.; Spitz, D. R. 2-Deoxy-D-glucose combined with cisplatin enhances cytotoxicity via metabolic oxidative stress in human head and neck cancer cells. Cancer Res. 67:3364–3370; 2007.
21. Weichselbaum, R. R.; Dahlberg, W.; Beckett, M.; Karrison, T.; Miller, D.; Clark, J.; Ervin, T. J. Radiation-resistant and repair-proficient human tumor cells may be associated with radiotherapy failure in head- and neck-cancer patients. Proc. Natl. Acad. Sci. USA 83:2684–2688; 1986.
22. Spitz, D. R.; Malcolm, R. R.; Roberts, R. J. Cytotoxicity and metabolism of 4-hydroxy-2-nonenal and 2-nonenal in H2O2-resistant cell lines. Do aldehydic by-products of lipid peroxidation contribute to oxidative stress? Biochem. J. 267:453–459; 1990.
23. Hidalgo, M.; Siu, L. L.; Nemunaitis, J.; Rizzo, J.; Hammond, L. A.; Takimoto, C.; Eckhardt, S. G.; Tolcher, A.; Britten, C. D.; Denis, L.; Ferrante, K.; Von Hoff, D. D.; Silberman, S.; Rowinsky, E. K. Phase I and pharmacologic study of OSI-774, an epidermal growth factor receptor tyrosine kinase inhibitor, in patients with advanced solid malignancies. J. Clin. Oncol. 19:3267–3279; 2001.
24. Sobhakumari, A.; Schickling, B. M.; Love-Homan, L.; Raeburn, A.; Fletcher, E. V.; Case, A. J.; Domann, F. E.; Miller, F. J., Jr.; Simons, A. L. NOX4 mediates cytoprotective autophagy induced by the EGFR inhibitor erlotinib in head and neck cancer cells. Toxicol. Appl. Pharmacol. 272:736–745; 2013.
25. Mohanti, B. K.; Rath, G. K.; Anantha, N.; Kannan, V.; Das, B. S.; Chandramouli, B. A.; Banerjee, A. K.; Das, S.; Jena, A.; Ravichandran, R.; Sahi, U. P.; Kumar, R.; Kapoor, N.; Kalia, V. K.; Dwarakanath, B. S.; Jain, V. Improving cancer radiotherapy with 2-deoxy-D-glucose: Phase I/II clinical trials on human cerebral gliomas. Int. J. Radiat. Oncol. Biol. Phys. 35:103–111; 1996.
26. Xi, H.; Barredo, J. C.; Merchan, J. R.; Lampidis, T. J. Endoplasmic reticulum stress induced by 2-deoxyglucose but not glucose starvation activates AMPK through CaMKKbeta leading to autophagy. Biochem. Pharmacol. 85:1463–1477; 2013.
27. Xi, H.; Kurtoglu, M.; Liu, H.; Wangpaichitr, M.; You, M.; Liu, X.; Savaraj, N.; Lampidis, T. J. 2-Deoxy-D-glucose activates autophagy via endoplasmic reticulum stress rather than ATP depletion. Cancer Chemother. Pharmacol. 67:899–910; 2011.
28. Zagorodna, O.; Martin, S. M.; Rutkowski, D. T.; Kuwana, T.; Spitz, D. R.; Knudson, C. M. 2-Deoxyglucose-induced toxicity is regulated by Bcl-2 family members and is enhanced by antagonizing Bcl-2 in lymphoma cell lines. Oncogene 31:2738–2749; 2012.
29. Contessa, J. N.; Bhojani, M. S.; Freeze, H. H.; Rehemtulla, A.; Lawrence, T. S. Inhibition of N-linked glycosylation disrupts receptor tyrosine kinase signaling in tumor cells. Cancer Res. 68:3803–3809; 2008.
30. Yoon, S. J.; Nakayama, K.; Hikita, T.; Handa, K.; Hakomori, S. I. Epidermal growth factor receptor tyrosine kinase is modulated by GM3 interaction with N-linked GlcNAc termini of the receptor. Proc. Natl. Acad. Sci. USA 103:18987–18991; 2006.
31. Schiavi, A.; Maglioni, S.; Palikaras, K.; Shaik, A.; Strappazzon, F.; Brinkmann, V.; Torgovnick, A.; Castelein, N.; De Henau, S.; Braeckman, B. P.; Cecconi, F.; Tavernarakis, N.; Ventura, N. Iron-starvation-induced mitophagy mediates lifespan extension upon mitochondrial stress in C. elegans. Curr. Biol. 25:1810–1822; 2015.
32. Guan, X.; Qian, Y.; Shen, Y.; Zhang, L.; Du, Y.; Dai, H.; Qian, J.; Yan, Y. Autophagy protects renal tubular cells against ischemia/reperfusion injury in a time-dependent manner. Cell. Physiol. Biochem. 36:285–298; 2015.
33. Shen, Y.; Yang, J.; Zhao, J.; Xiao, C.; Xu, C.; Xiang, Y. The switch from ER stress-induced apoptosis to autophagy via ROS-mediated JNK/p62 signals: A survival mechanism in methotrexate-resistant choriocarcinoma cells. Exp. Cell Res. 334:207–218; 2015.
34. Jeon, J. Y.; Kim, S. W.; Park, K. C.; Yun, M. The bifunctional autophagic flux by 2-deoxyglucose to control survival or growth of prostate cancer cells. BMC Cancer 15:623; 2015.
35. Kim, S. E.; Park, H. J.; Jeong, H. K.; Kim, M. J.; Kim, M.; Bae, O. N.; Baek, S. H. Autophagy sustains the survival of human pancreatic cancer PANC-1 cells under extreme nutrient deprivation conditions. Biochem. Biophys. Res. Commun. 463:205–210; 2015.
36. Suzuki, M.; O'Dea, J. D.; Suzuki, T.; Agar, N. S. 2-Deoxyglucose as a substrate for glutathione regeneration in human and ruminant red blood cells. Comp. Biochem. Physiol. B 75:195–197; 1983.
37. Ahmad, I. M.; Aykin-Burns, N.; Sim, J. E.; Walsh, S. A.; Higashikubo, R.; Buettner, G. R.; Venkataraman, S.; Mackey, M. A.; Flanagan, S. W.; Oberley, L. W.; Spitz, D. R. Mitochondrial O2.- and H2O2 mediate glucose deprivation-induced stress in human cancer cells. J. Biol. Chem. 280:4254–4263; 2005.
38. Coleman, M. C.; Asbury, C. R.; Daniels, D.; Du, J.; Aykin-Burns, N.; Smith, B. J.; Li, L.; Spitz, D. R.; Cullen, J. J. 2-Deoxy-D-glucose causes cytotoxicity, oxidative stress, and radiosensitization in pancreatic cancer. Free Radic. Biol. Med. 44:322–331; 2008.
39. Hadzic, T.; Aykin-Burns, N.; Zhu, Y.; Coleman, M. C.; Leick, K.; Jacobson, G. M.; Spitz, D. R. Paclitaxel combined with inhibitors of glucose and hydroperoxide metabolism enhances breast cancer cell killing via H2O2-mediated oxidative stress. Free Radic. Biol. Med. 48:1024–1033; 2010.
40. Fath, M. A.; Diers, A. R.; Aykin-Burns, N.; Simons, A. L.; Hua, L.; Spitz, D. R. Mitochondrial electron transport chain blockers enhance 2-deoxy-D-glucose induced oxidative stress and cell killing in human colon carcinoma cells. Cancer Biol. Ther. 8:1228–1236; 2009.
41. Rutkowski, D. T.; Kaufman, R. J. A trip to the ER: Coping with stress. Trends Cell Biol. 14:20–28; 2004.
42. Ling, Y. H.; Li, T.; Perez-Soler, R.; Haigentz, M., Jr. Activation of ER stress and inhibition of EGFR N-glycosylation by tunicamycin enhances susceptibility of human non-small cell lung cancer cells to erlotinib. Cancer Chemother. Pharmacol. 64:539–548; 2009.
43. Fernandes, H.; Cohen, S.; Bishayee, S. Glycosylation-induced conformational modification positively regulates receptor-receptor association: A study with an aberrant epidermal growth factor receptor (EGFRvIII/DeltaEGFR) expressed in cancer cells. J. Biol. Chem. 276:5375–5383; 2001.
44. Kim, S. M.; Yun, M. R.; Hong, Y. K.; Solca, F.; Kim, J. H.; Kim, H. J.; Cho, B. C. Glycolysis inhibition sensitizes non-small cell lung cancer with T790M mutation to irreversible EGFR inhibitors via translational suppression of Mcl-1 by AMPK activation. Mol. Cancer Ther. 12:2145–2156; 2013.